Journal of Atmospheric Chemistry
https://doi.org/10.1007/s10874-022-09430-7

Long-range transport of Asian emissions to the West Pacific tropical tropopause layer

Victoria Treadaway[1] · Elliot Atlas[1] · Sue Schauffler[2] · Maria Navarro[1] · Rei Ueyama[3] · Leonhard Pfister[3] · Troy Thornberry[4] · Andrew Rollins[4] · James Elkins[5] · Fred Moore[5] · Karen Rosenlof[4]

Received: 19 May 2021 / Accepted: 21 January 2022

Abstract

Rapid transport by deep convection is an important mechanism for delivering surface emissions of reactive halocarbons and other trace species to the tropical tropopause layer (TTL), a key region of transport to the stratosphere. Recent model studies have indicated that increased delivery of short-lived halocarbons to the TTL could delay stratospheric ozone recovery. We report here measurements in the TTL over the western Pacific Ocean of short-lived halocarbons and other trace gases that were transported eastward after convective lofting over Asia. Back-trajectories indicate the sampled air primarily originated from the Indian subcontinent. While short-lived organic bromine species show no measurable change over background mixing ratios, short-lived chlorinated organic species were elevated above background mixing ratios (dichloromethane (Δ48.2 ppt), 1,2-dichloroethane (Δ4.21 ppt), and chloroform (Δ4.85 ppt)), as well as longer-lived halogenated species, methyl chloride (Δ82.0 ppt) and methyl bromide (Δ1.91 ppt). This transported air mass thus contributed an excess equivalent effective chlorine burden of 316 ppt, with 119 ppt from short lived chlorinated species, to the TTL. Non-methane hydrocarbons (NMHC) were elevated 60 - 400% above background mixing ratios. The NMHC measurements were used to characterize the potential source regions, which are consistent with the convective influence analysis. The measurements indicate a chemical composition heavily impacted by biofuel/biomass burning and industrial emissions. This work shows that convection can loft Asian emissions, including short-lived chlorocarbons, and transport them to the remote TTL.

Keywords Asian emissions · Chlorinated very-short lived substances · Tropical upper troposphere · Long-range transport

Maria Navarro: deceased.

✉ Victoria Treadaway
victoria.treadaway@rsmas.miami.edu

Extended author information available on the last page of the article

1 Introduction

The chemical composition of the tropical upper troposphere (UT) and tropical tropopause layer (TTL) is influenced by emissions in the surface boundary layer and subsequent vertical and horizontal transport mechanisms (e.g. Ashfold et al. 2015; Donets et al. 2018; Filus et al. 2020; Vogel et al. 2019). The reactive trace gases deposited into the TTL can transit into the lower stratosphere, with potential impacts on ozone and radiative properties (Levine et al. 2007). Relatively few in-situ measurements of trace gases in the TTL are available to characterize the magnitude and variability of the chemical composition in this important region of the atmosphere. This paper addresses one of the transport pathways to the TTL and quantifies the chemical perturbation associated with this transport. We combine back-trajectory and convective influence analysis with interpretation of trace gas ratios to identify the major source region of emissions that were transported to the TTL of the western Pacific. Of particular relevance is the observed increase in reactive organic halogen species which are important to the overall halogen loading of the stratosphere.

Anthropogenic emissions of chlorinated very short-lived substances (VSLS), i.e., those which have tropospheric lifetimes less than 6 months, are rising (Engel et al. 2018; Fang et al. 2019; Hossaini et al. 2019, 2017; Oram et al. 2017). No similar temporal trend in brominated VSLS has been observed, as these are primarily from natural marine sources. Model studies, though, have suggested a small positive trend in Br at the cold point of 0.04 ± 0.015 ppt/decade at 17 km over the Indian Ocean (Tegtmeier et al. 2020). VSLS are not included in the Montreal Protocol because they are short-lived and play a minor role in stratospheric ozone destruction compared to CFCs (Engel et al. 2018). Ozone depletion potential (ODP) describes a compound's effectiveness to destroy ozone in relation to CFC-11, a reference compound given an ODP of 1.0 (Solomon and Albritton 1992; Wuebbles et al. 1983). VSLS ODPs are substantially lower than longer lived compounds and range from approximately 0.003 to 0.025 (Claxton et al. 2019). Due to the short lifetimes, VSLS ODPs are dependent on transport time and tropospheric lifetime. As a result, VSLS originating in the tropics, Indian subcontinent, and southeast Asia have the greatest ODP in the lower stratosphere as a result of convection which drastically shortens transport time to the upper troposphere (Brioude et al. 2010; Claxton et al. 2019; Pisso et al. 2010). Orbe et al. (2015) found that roughly half of the air in the tropical lower stratosphere originated from the Northern Hemisphere (NH) boundary layer (BL) during NH fall and winter. Annually, of this NH air, 55–75% is from the subtropical BL (10°N—25°N) and 25–45% from the Asian continent north of 25°N (Orbe et al. 2015). Considering the significant fraction of air in the tropical lower stratosphere that originates from Asia, it is important to better understand the chemical composition and impact of BL emissions that are lofted to the UT.

Nearly 90% of the chlorinated VSLS in the upper TTL (15.5 – 16.5 km) are derived from anthropogenic sources (Engel et al. 2018). As of the latest assessment, chlorinated VSLS make up only 3.5% of the total chlorine source gas injected into the stratosphere (Engel et al. 2018). As Montreal Protocol controlled halocarbons decrease and VSLS usage increases, the proportion of VSLS in the stratosphere will increase, which could delay ozone hole recovery time (Fang et al. 2019; Hossaini et al. 2017; Oram et al. 2017). The three major chlorinated VSLS are dichloromethane (CH_2Cl_2, tropospheric lifetime (τ) ~ 144 days), chloroform ($CHCl_3$, τ ~ 149 days), and 1,2-dichloroethane (CH_2ClCH_2Cl, τ ~ 65 days). Dichloromethane, chloroform, and 1,2-dichloroethane contribute 70%, 18%, and 9% respectively to the chlorinated VSLS source gas injected into the stratosphere (Hossaini et al. 2019). Assuming no further growth in emissions, dichloromethane or

chloroform could delay the ozone hole recovery by 5 and 0.4 years respectively (Fang et al. 2019; Hossaini et al. 2017).

1,2-Dichloroethane is produced as a chemical feedstock, with 80–90% for vinyl chloride (Oram et al. 2017). It is also a cleaning/degreasing agent and fumigant (EPA 2020; Oram et al. 2017) and there is a small possible biomass burning source (Simpson et al. 2011). Dichloromethane uses include paint removal, metal cleaning/degreasing, blowing agent in foam production, and chemical feedstock for producing hydrofluorocarbons, Montreal Protocol replacement chemicals (Feng et al. 2018; Hossaini et al. 2017; Montzka et al. 2011). About half of chloroform originates from anthropogenic sources, primarily HCFC-22 and fluoropolymers production, though it is also emitted as a by-product in water chlorination and paper manufacturing (Montzka et al. 2011).

Recent work highlights the significance of convection for transporting Asian emissions, particularly halocarbons, to the upper troposphere and the growing impact of chlorinated VSLS on stratospheric ozone (Adcock et al. 2020; Ashfold et al. 2015; Claxton et al. 2019; Fang et al. 2019; Hossaini et al. 2019, 2017; Oram et al. 2017; Orbe et al. 2015; Pisso et al. 2010; Umezawa et al. 2014). Here we report measurements of VSLS, methyl halides, and non-methane hydrocarbons (NMHC) over the Western Pacific during the 2016 NASA Pacific Oxidants, Sulfur, Ice, Dehydration, and cONvection (POSIDON) mission (https://espo.nasa.gov/posidon/content/POSIDON_0) that show evidence of rapid vertical transport to the TTL. Back-trajectories and chemical signatures suggest this air was lofted from the Indian subcontinent 6–10 days prior to sampling on 19 October (Research Flight 5). Though brominated VSLS contribute to halogen reactivity in the UT and TTL, we focus here on chlorinated VSLS due to their recent increases in atmospheric abundances, their observed enhancement over background levels, and the potential impact on stratospheric ozone as mentioned above. In this case, the transported air masses also contain significant enhancements of longer-lived halocarbons (CH_3Cl and CH_3Br) from biomass/biofuel emissions, which further impact ozone chemistry in the TTL and lower stratosphere.

1.1 Sampling and methods

The POSIDON mission was conducted from Guam from 12 - 30 October 2016 using the NASA WB-57 aircraft. Figure 1 shows the locations of the whole air samples along the flight track for the 10 research flights (RF). There were 460 whole air samples collected during POSIDON, approximately 50 per flight. Most flights were oriented along a westerly/southwesterly or easterly track. Two flights (RF06 and RF09) went south across the equator to approximately 2°S. The typical flight pattern included multiple vertical profiles between roughly 14 – 18 km. Temperature, pressure, and altitude measurements were measured by the WB-57 Meteorological Measurement System (MMS).

Whole air sampler (WAS) samples were pressurized to approximately 40–50 psia into 1.3 L electropolished stainless steel canisters using a 4-stage metal bellows pump. Sample canisters were cleaned prior to flight by repeated evacuation to approximately 20 mTorr and flushed with wet nitrogen. After the final evacuation, 8 torr of water vapor was added to each canister to passivate the canister interior surface. Typical canister fill times ranged from ~ 30 s at 14 km altitude to 90 s at 19 km altitude. Canisters were set to open in a sequence controlled by the WB57 "backseater", with either a 'fast' or 'slow' interval between canisters that was decided before flights depending on profile maneuvers. For example, during RF05 the slow interval was 350 s between canister open times with an average canister fill time of 58 s.

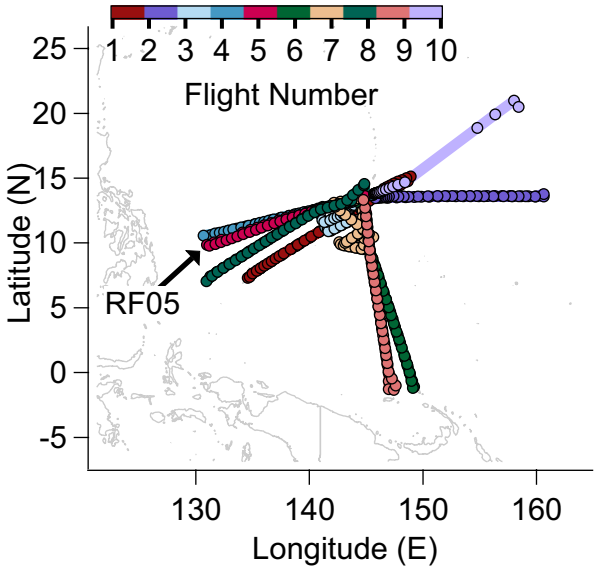

Fig. 1 Map of whole air samples (WAS) collected along the flight tracks colored by flight number

The RF05 fast interval averaged 150 s and was only used during the final descent back to the Guam airport.

After flights, samples were shipped to the University of Miami and analysis was performed within two to three weeks of collection, e.g. RF05 was sampled on 19 October and analyzed on 4–6 November. Sample analysis was performed on a multi-channel GC/MS/FID/ECD system (Agilent 7890 GC, 5973 MS), which used a Markes Unity system for sample concentration. Method details are described in Andrews et al. (2016) and Schauffler et al. (1999). Forty-seven chemical species were measured including halocarbons, hydrocarbons, and other volatile organic compounds. Uncertainties vary between 2 and 20% for individual compounds. Standard scales are described in Schauffler et al. (1999) and Flocke et al. (1999). Standards included in house prepared gravimetric standards as well as standard mixing ratios calibrated against NIST standards using gas chromatography/atomic emission detection. Examples of standard comparisons include Hall et al. (2014) and Andrews et al. (2016), in addition to unpublished comparisons between major labs.

Other trace gas measurements used in this analysis include ozone, carbon monoxide, and sulfur dioxide. Ozone was measured using a dual-beam UV absorption photometer (Gao et al. 2012). Carbon monoxide was measured with an in situ GC/ECD system (Wofsy 2011). Sulfur dioxide was measured with laser-induced fluorescence as described by Rollins et al. (2016, 2018). High frequency data was averaged over the WAS canister fill times.

The diabatic trajectories are calculated using horizontal winds and radiative heating rates from the 6-hourly ERA-Interim reanalysis data (0.5 deg latitude × 0.5 deg longitude resolution and 60 vertical levels). Instead of linear interpolation, the ERA-Interim data are properly interpolated between vertical levels using Fourier analysis to recover the degraded wave-driven variability in the tropical tropopause layer (Kim and Alexander 2013).

Global, three-hourly fields of convective cloud top height are estimated from geostationary satellite imagery of brightness temperatures combined with GPM/TRMM rainfall measurements (Pfister et al. 2010; Ueyama et al. 2015). Briefly, we first search for grid points exceeding a threshold of 9 mm/hr over land or 1.5 mm/hr over ocean. Minimum

brightness temperatures within a search distance of 0.25 degrees from the center of the selected grid cells are then noted. Cloud top altitude is derived from the altitude of the brightness temperature in the "mixed' temperature profile that accounts for the mixing of convectively lofted air with the environment (i.e., calculated by assuming a mixture of 30% environmental air and 70% air lifted adiabatically from the tropopause). In the final step, the derived altitude is raised by 1 km to account for the known underestimation of cloud top altitudes calculated via infrared methods compared to lidar methods (Sherwood et al. 2004). This approach to estimating the impact of convection on the humidity and cirrus clouds in the TTL has been successfully employed in previous studies (e.g., Schoeberl et al. 2018; Ueyama et al. 2018, 2015).

Ratios of NMHC were used to characterize the enhanced trace gas measurements and compared to literature values for source trace gas compositions. For WAS internal consistency, rather than using carbon monoxide as a reference gas (e.g. Baker et al. 2011), we used the ratio of alkanes to ethyne. For alkanes with longer (shorter) lifetimes than ethyne, the ratio will increase (decrease) over time as ethyne is oxidized more quickly (slowly) than the alkane. Because a trace gas source composition will change during transport and photochemical processing, we use the following simplified relationship to estimate how the alkane to ethyne ratio above background levels might have evolved to reach observed values

$$\left[\frac{X_n}{X_{ethyne}}\right]_0 = \left[\frac{X_n}{X_{ethyne}}\right]_t * e^{((k_x - k_{ethyne})[OH]t)} \quad (1)$$

where X_n = mixing ratio of the alkane; X_{ethyne} = mixing ratio of ethyne; k = rate constant with OH radical; [OH] = average number density of OH radical; t = transit time. For our calculation we used [OH] = 1.46×10^6 molecules cm^{-3}, the modeled tropical tropospheric average calculated in Lelieveld et al. (2016), and rate constants evaluated at 230 K. Rate constants for ethane, ethyne, propane, and n-butane were 9.00×10^{-14} cm^3 $molecule^{-1}$ s^{-1}, 4.58×10^{-13} cm^3 $molecule^{-1}$ s^{-1}, 5.98×10^{-13} cm^3 $molecule^{-1}$ s^{-1}, and 1.57×10^{-12} cm^3 $molecule^{-1}$ s^{-1}, respectively (Atkinson 2003; Atkinson et al. 1997). The choice of 230 K to represent upper troposphere air assumes no reaction with OH from the surface to cloud top, which is reasonable given that the gases are lofted to the upper troposphere via convection much faster than typical lifetimes for the gases examined here. This estimation also assumes there is no mixing with background air which would reduce the ratios reported here. Finally, the OH mixing ratio we use for calculations does not factor in the reported OH minimum in the tropical West Pacific (Rex et al. 2014). The impact of these assumptions is discussed in Sect. 2.3.

2 Results and discussion

2.1 Trace gas variations

While the focus here is on the impact of Asian emissions in the TTL, we first briefly describe the trace gas composition observed during the full POSIDON mission to provide context for the observations of Asian pollution in the region. The variation of NMHC and non-marine halocarbons along the POSIDON flight path generally followed a pattern expected for the NH remote atmosphere with low levels of hydrocarbons and halocarbons at locations far removed from continental sources (e.g., Simmonds et al. 2006; Yates et al.

2010; AGAGE database (http://agage.mit.edu/data; Prinn et al. 2018); NOAA Halocarbons and other Trace Species database (https://www.esrl.noaa.gov/gmd/hats/)).

Figure 2 shows potential temperature vertical profiles for selected trace gases measured during POSIDON. The TTL, highlighted in yellow in Fig. 2 and Fig. S1, is between 150 hPa (~355 K) and 70 hPa (~425 K) as defined in Fueglistaler et al. (2009). Throughout the mission, long-lived trace gases (CFCs, HCFCs) had uniform mixing ratios in the upper troposphere (Fig. 2d, e). Small decreases in mixing ratio at the top of the vertical profiles were associated with stratospheric influence in the TTL. These variations were accompanied by a significant increase in ozone (Fig. 2a). Long-lived trace gases decreased ~5 – 15% below upper troposphere background levels when ozone increased by several hundred ppb.

We identify two main processes that modify trace gas composition during POSIDON: recent convection and long-range transport of Asian emissions. Consistent with marine convective transport, trace gases of oceanic origin maximized in the lower altitudes of the flight profiles corresponding to the main convective outflow. In several flights, mixing ratios of bromoform, a short-lived marine species, (Fig. 2l) were above detection limits (0.14 ppt) only at the lowest altitudes of the vertical profiles. Short-lived marine emissions were detected more frequently during the first four research flights compared to later in the mission. Marine emissions with longer lifetimes, such as dibromomethane (Fig. 2k), were most abundant at altitudes ≤ 14 km though remained detectable at higher altitudes with monotonically decreasing mixing ratios.

Tegtmeier et al. (2012) reported emission-based estimates for bromoform and dibromomethane mixing ratios at 17 km (representative of the cold point) using FLEXPART and sea-to-air emission fluxes measured during the TransBrom cruise. The TransBrom R/V *Sonne* research cruise made a meridional transect (146°E) in the West Pacific Ocean from Japan to Australia in October 2009 (Krüger and Quack 2013). We found reasonable agreement with the Tegtmeier et al. estimate for bromoform. Tegtmeier et al. (2012) reported an average of ~0.23 ppt Br source gas, assuming wet deposition, from bromoform and we report 0.15 ppt Br from bromoform (averaged from 17–17.5 km, ~375–380 K potential temperature). We found higher dibromomethane at 17 km (averaged from 17–17.5 km, ~375–380 K potential temperature, 0.6 ppt Br) than their reported average (~0.10 ppt Br), though this is within the range reported. Both Tegtmeier et al. (2012) and POSIDON measurements were lower than the tropical tropopause average (1.28 ppt Br, 16.5 – 17.5 km, 375–385 K) based on upper atmospheric measurements (Engel et al. 2018). Tegtmeier et al. (2012) measured low CH_2Br_2 flux from the ocean leading to the lower reported upper atmospheric measurements available at the time. They suggest that other oceanic regions are more important for dibromomethane stratospheric budget. Similar analyses of oceanic contribution to brominated VSLS transport to the TTL during the November time period in the West Pacific was reported in Ashfold et al. (2012). They identified major potential source regions of marine boundary layer air to the TTL over Borneo primarily from the equatorial Pacific Ocean, though a small fraction of trajectories were identified from the northern Bay of Bengal.

The study region was also influenced by a typhoon during the POSIDON mission. Typhoon Haima developed in the area south and west of Guam, reaching maximum intensity (Category 5) on 19 October coinciding with RF05 (Rollins et al. 2018). The typhoon lofted marine emissions that were sampled at the westernmost portions of RF04 (18 October) and RF05, which were closest to the influence of Typhoon Haima (Fig. S2). Elevated bromoform is evident at the western edge of the flight track corresponding to Typhoon Haima during RF04 and RF05 (Fig. S3) with evidence of more lofting during RF04. The lofted bromoform at the eastern edge of the RF04 flight track is from slightly older

convection (2–3 days before sampling) and not the result of updraft from the typhoon core. It is possible there was isolated convection in the vicinity as the typhoon was forming.

Despite the nearly identical flight path for RF04 and RF05 and the proximity of Typhoon Haima, the RF04 ozone and ethyne profiles were more comparable to the equatorial flight RF06 than RF05 (Fig. S4). RF04 was characteristic of a remote tropical airmass identified by lower levels of ozone and ethyne (as well as short-lived chlorinated VSLS) that was influenced by the typhoon. For example, methyl iodide, an oceanic tracer with a short lifetime (3.5 days), was elevated for RF04 relative to RF05 indicating recent convection. Bromoform was also greater below 15 km for RF04 relative to RF05 (Figs. S3 and S4). Previous work predicted enhanced methyl iodide and bromoform at the cold point due to typhoon vertical uplift (Tegtmeier et al. 2013, 2012). During RF04, we observed elevated methyl iodide and bromoform related to Typhoon Haima in the TTL but below the cold point. Dibromomethane was similar during all three flights, which we ascribe to a combination of factors: 1) dibromomethane has relatively less variability compared to bromoform in the marine boundary layer (e.g. Brinckmann et al. 2012; Fuhlbrügge et al. 2016; Liu et al. 2011; Quack et al. 2007) and 2) the longer lifetime of dibromomethane suggests that it will be better mixed through the atmosphere.

2.2 Long-range transport

A notable exception to the remote atmosphere composition was found during RF05, where we observed anomalously high levels of many trace gases with primarily anthropogenic/continental sources (Fig. 2, red markers), and no enhancement of marine derived VSLS. During RF05, we observed a layer of elevated trace species in the TTL between 14 and 16 km altitude, or approximately 360 – 370 K potential temperature.

RF05 had much higher mixing ratios for both ozone and ethyne, a combustion tracer, at 360 K compared to the tropical background. Mixing ratios for long-lived anthropogenic halogenated species, CFCs and HCFCs, were similar to the rest of the campaign. Notable exceptions are apparent for anthropogenic, short-lived halogens (Fig. 2f-h) and hydrocarbons (Fig. 2b, c) as well as methyl chloride and methyl bromide (Fig. 2i and j). The RF05 enhancements above background mixing ratios, defined as the 25th percentile after removing stratospheric samples (Barletta et al. 2009), for a selection of trace gases are presented in Table 1. Ozone and carbon monoxide were elevated Δ46.9 ppb and Δ32.9 ppb above background mixing ratios. Smaller, but significant, enhancements were found for the longer-lived gases, including methane (Δ72.0 ppb), methyl chloride (Δ82.0 ppt) and methyl bromide (Δ1.91 ppt). Given the recent interest in the increasing role of short-lived halocarbons on stratospheric ozone (Fang et al. 2019; Hossaini et al. 2017; Oram et al. 2017), the observed increases in chlorinated VSLS, dichloromethane (Δ48.2 ppt), 1,2-dichloroethane (Δ4.21 ppt), and chloroform (Δ4.85 ppt), are particularly significant.

Rollins et al. (2018) noted enhancements of SO_2 (40–70 ppt) during RF04 associated with Typhoon Haima but similar magnitude mixing ratios were not measured during the RF05 sortie near Haima outflow. Still, the trend and variation in SO_2 during RF05 between 360 and 370 K closely followed the patterns for NMHC (Fig. S5) suggesting a measurable anthropogenic contribution to the observed SO_2 during RF05. The main sources of SO_2 include coal/fuel combustion, volcanoes, and marine sources (Rollins et al. 2018 and references therein).

Table 1 RF05 trace gas average enhancements above background mixing ratios measured between 14–16 km. Background is defined as the 25th percentile after removing stratospheric samples. Mixing ratio is ppt unless indicated otherwise

Chemical Species	Background Mixing Ratio	Plume Average Mixing Ratio	Δ Mixing Ratio Above Background	% Increase Above Background
Ozone (ppb)	16.9	63.8	46.9	277
Methane (ppb)	1832	1904	72.0	3.93
Ethane	281	489	208	74.0
Ethyne	30.8	105	74.2	241
Propane	11.6	60.3	48.7	420
n-butane	1.85	7.38	5.53	299
Methyl Chloride	542	624	82.0	15.1
Methyl Bromide	6.67	8.58	1.91	28.6
Dichloromethane	41.6	89.8	48.2	115
Chloroform	7.85	12.7	4.85	61.8
Dichloroethane	6.99	11.2	4.21	60.2

Figure 3 shows the back-trajectory analysis for the WAS samples with elevated NMHC and halocarbon mixing ratios between 14–16 km with one trajectory per canister sample location. The trajectories shown in the figure stop at the most recent point of convective influence (Fig. 3, circles). Most trajectories originated over the Bay of Bengal and the Indian subcontinent approximately 6–8 days before sampling. Consistent with the convective influence analysis, satellite images (Fig. S6) confirm that this region was convectively active during this period. For this season, it is likely the air lofted over the bay originated from the Indian subcontinent. Mallik et al. (2014) reported post-monsoonal winds travel across the Indo-Gangetic Plain (IGP) out to the Bay of Bengal. Sahu et al. (2006) sampled elevated alkane mixing ratios during a cruise in the Bay of Bengal in September and October 2002 and reported air originated from Chennai and Sri Lanka. A small fraction of sampled air masses originated in the South China Sea approximately 10–12 days before sampling (Fig. 3, gray lines) and passed over the Bay of Bengal. Based on back-trajectories, the air masses likely mixed since traveled a similar path and altitude range as the Bay of Bengal air mass (Fig. S7, dashed lines). Further, there is no clear chemical distinction in halocarbons or hydrocarbons (all within 1σ) between these South China Sea and India/Bay of Bengal samples. The sampled continental plume is treated as originating from the Bay of Bengal and Indian subcontinent though there was likely mixing with East Asian air as seen in the chemical characterization discussed below. Oceanic VSLS emissions would also be entrained during convection over the Bay of Bengal. Fiehn et al. (2018) model the seasonal entrainment of oceanic emissions to the stratosphere and demonstrate the seasonality of transport and emissions as major factors regulating the delivery of marine emissions to the TTL. Major entrainment over the Indian Ocean was found to occur in the JJA summer period, with lesser contribution during the autumn. The lack of enhanced brominated VSLS observed during POSIDON RF05 suggests that ocean emissions were not exceptional at the location and time of the convection. Further, Tegtmeier et al. (2020) discuss the

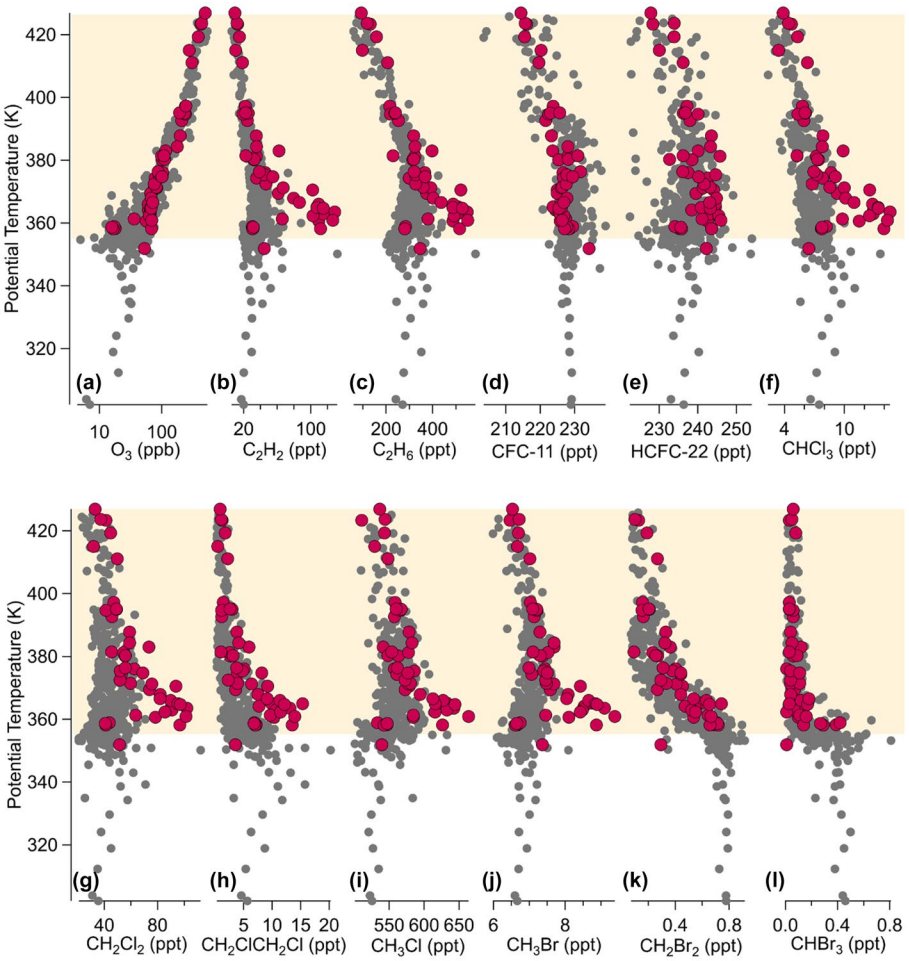

Fig. 2 Potential temperature (K) vertical profiles for (**a**) ozone (O_3, ppb), (**b**) ethyne (C_2H_2, ppt), (**c**) ethane (C_2H_6, ppt), (**d**) CFC-11 (ppt), (**e**) HCFC-22 (ppt), (**f**) chloroform ($CHCl_3$, ppt), (**g**) dichloromethane (CH_2Cl_2, ppt), (**h**) dichloroethane (CH_2ClCH_2Cl, ppt), (**i**) methyl chloride (CH_3Cl, ppt), (**j**) methyl bromide (CH_3Br, ppt), (**k**) dibromomethane (CH_2Br_2, ppt), and (**l**) bromoform ($CHBr_3$, ppt). Red circles are for RF05 on 19 October and gray circles are the whole air samples for the other nine flights. Ozone samples were averaged over the whole air sample collection time for each canister and are shown on a log scale

complexities and uncertainties associated with understanding air–sea coupling in the Indian Ocean region.

2.3 Chemical source characterization

By using tracer correlations and ratios, we should be able to relate the relative chemical composition of the enhanced trace gas layer to different source types, including urban, biomass, and biofuel emissions and potentially to different regions of Asia. (e.g., Baker et al. 2011; Barletta et al. 2009; de Gouw et al. 2001; Manö & Andreae 1994; Santee et al. 2013;

Simpson et al. 2011; Umezawa et al. 2014). However, we are limited by the lack of seasonally resolved Asian measurements of both NMHC and halocarbons in these different source environments. The NMHC database is more extensive than for halocarbons in the region, thus we use NMHC ratios to discuss potential airmass origin, but we also compare our halocarbon measurements to recent and relevant literature results.

The NMHC ratios for POSIDON RF05 WAS samples were age-corrected (Eq. 1) for 6, 8, and 10-day processing, which should account for convective transport time. The age-corrected ratios should reflect the source composition at the beginning of the trajectory either 6, 8, or 10 days prior to sampling. Table 2 includes NMHC values from literature reports from India or China that are within one standard deviation of the age-corrected POSIDON samples. Table S1 includes all literature values the POSIDON plume was evaluated against. The closest match for ethane and propane ratios were measurements from the IGP and the Himalayas. The remaining sites with near matches to the flight data had ethane/ethyne and propane/ethyne ratios within one standard deviation of the POSIDON age-corrected ratios. These include rural sites in China, Asian monsoon outflow measurements near India, and biofuel emissions.

NMHC measurements from rural China reported in Tang et al. (2009) were the only literature samples within one standard deviation for all three ratios. The Yangtze River Delta rural site in Tang et al. (2009) best matched POSIDON measurements and is considered a background site in China. However, it is influenced by urban and industrial emissions from distant cities, such as Shanghai (210 km from the site), as well as local (2–10 km from the site) urban emissions (Tang et al. 2009). It is also impacted by the less populated mountainous regions thus it is a mixed rural site. Other work from this site attributed 71% of VOCs sampled to a mixture of vehicle emissions and biofuel (Guo et al. 2004). While the closest match for all three ratios was from a Chinese site, the chemical characterization of the area may be more generally indicative of rural and developing areas in Asia.

RF05 age-corrected n-butane/ethyne ratios were lower than the remaining literature reported in Table 2. The estimated atmospheric lifetime for n-butane at 230 K and $[OH] = 1.46 \times 10^6$ molecules cm^{-3} is 5 days which is less than the travel time determined by back-trajectories. There could have been a substantial loss of n-butane which would impact the ratios resulting in the underprediction reported here. Other caveats to consider for this analysis are that this assumes there is no mixing or chemical reaction besides reaction with OH, and our source ratios may be younger than what was transported as there is no emission change accounted for from the surface until the upper troposphere (230 K).

Another impact on the calculation to consider is the tropical West Pacific OH minimum (125°E to 140°E, Rex et al. (2014)). The peak of the reported minimum is centered over the equator and reaches up to ~ 10°N, near the RF05 flight track, in the same season as POSIDON. However, in-situ ozone measurements during POSIDON did not encounter the zero ozone levels reported from the ozonesonde measurements of Rex et al. (2014), which lead to the modeled "OH hole". Even so, we estimated NHMC ratios with the modeled OH minimum (0.7×10^6 molecules cm^{-3}) (Rex et al. 2014). While the ratios do change with the ethane/ethyne ratio increasing and the propane and n-butane ratios decreasing, it is still within one standard deviation of the reported results in Table 2 even with the unlikely assumption of being within an OH minimum for the entire transport time (6–8 days). Thus, any encounter of the Asian Plume with an OH minimum region would not alter our conclusions regarding NMHC ratios.

Elevated levels of ethyne plus C2 – C4 alkanes and halocarbons such as dichloromethane, 1,2-dichloroethane, chloroform, and methyl halides suggest a mixture of industrial and biomass burning/biofuel emissions (Fig. 4). All linear correlations presented

Table 2 Age-corrected NMHC ratios for POSIDON relevant Asian literature measurements

Study	Year Sampled	Season Sampled	Country	Sample Type	Ethane/ Ethyne	Propane/ Ethyne	n-Butane/ Ethyne
This Study	2016	October	–	Day of Sampling	2.78 ± 0.97	0.654 ± 0.22	0.0738 ± 0.027
			–	6 days	2.11 ± 0.74	0.727 ± 0.25	0.171 ± 0.062
			–	8 days	1.92 ± 0.67	0.753 ± 0.26	0.227 ± 0.081
			–	10 days	1.75 ± 0.61	0.780 ± 0.27	0.300 ± 0.11
Baker et al. (2011)	–	–	–	Biofuel	1.68	0.48	N/A
	2008	April—Dec	India	Distant	1.33	0.59	N/A
Lal et al. (2012)	2004	Dec	India	Urban	1.74	0.72	0.43
					1.85	0.72	0.49
Sarangi et al. (2016)	2009–2011	Sept – Nov	Himalayas	Remote	1.64	0.82	0.55
Guo et al. (2004)	2002–2003	Sept-Aug	China	Rural	1.31	0.63	0.43
Tang et al. (2009)	2004	April/May	China	Rural	1.21	0.6	0.33

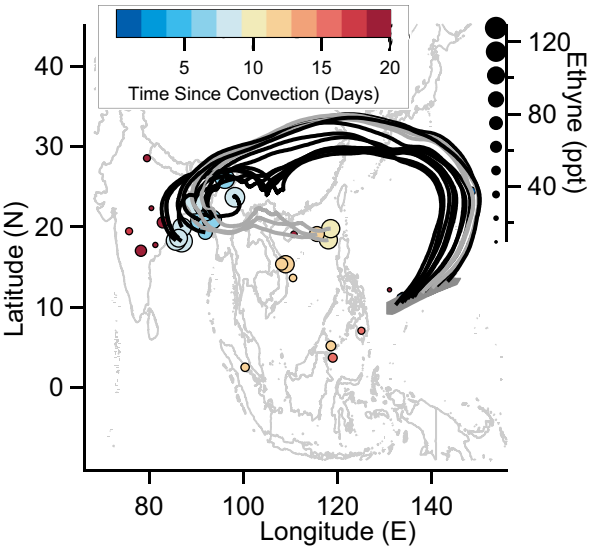

Fig. 3 Back-trajectories for the RF05 enhanced layer sampled between 14-16 km. Circles represent the back-trajectory convective endpoints for RF05 samples colored by time since convection at the time of sampling. Back-trajectories are presented only for the elevated WAS samples though there are back-trajectories available for each circle endpoint shown. Circles are sized by ethyne (ppt) mixing ratios. The RF05 flight track is in green

are statistically significant ($\alpha = 0.05$) except for HCFC-22 with chloroform (Fig. 4l). The HCFC-22 and chloroform correlation improves ($r^2 = 0.35$) and is statistically significant with the removal of a high $CHCl_3$ (12.92 ppt) and low HCFC-22 (238.4 ppt) point though this point is not statistically an outlier. Elevated methyl chloride (Δ82.0 ppt) and methyl bromide (Δ1.91 ppt) indicate contributions from biomass and/or biofuel burning (Butler 2000; Manö and Andreae 1994; Rudolph et al. 1995; Santee et al. 2013; Scheeren et al.

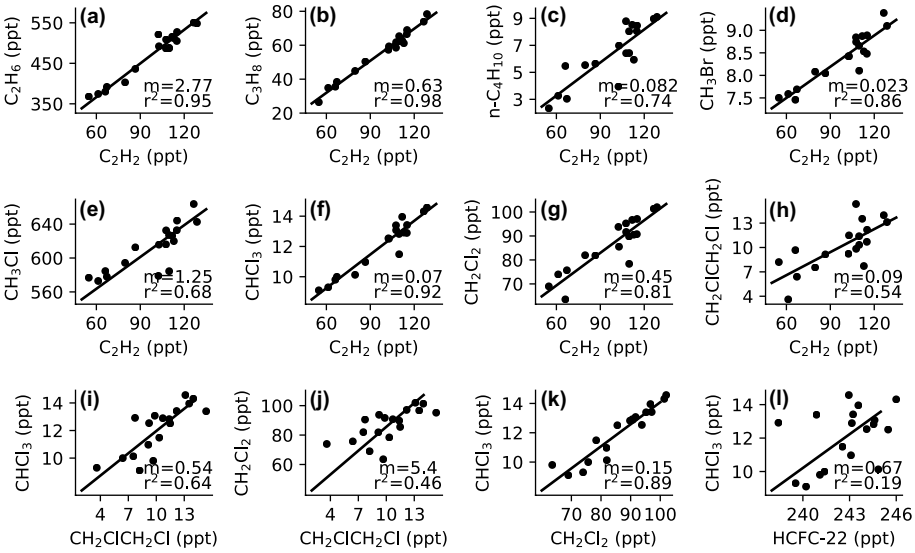

Fig. 4 Orthogonal Distance Regression (ODR) plots for ethyne with hydrocarbons and halocarbons (**a**-**h**) as well as between select halocarbons for the elevated plume encountered during RF05 (**i**-**l**). The squared Pearson correlation coefficient (r^2) and ODR slope (m) are included

2002; Simpson et al. 2011; Umezawa et al. 2014; Warwick et al. 2006), supported by the relationship with ethyne (Fig. 4e, $r^2 = 0.68$ and d, $r^2 = 0.86$ respectively). Satellite imagery indicates fires on the IGP during this period (red dots, Fig. S6). Lai et al. (2010) reported similar enhancements for both methyl chloride (Δ75.5 ppt) and methyl bromide (Δ1.8 ppt) from CARIBIC flights impacted by biomass and/or biofuel burning. The CARIBIC airmasses originated from the Indochinese Peninsula and ~ 54–92% of CO enhancements were linked to biomass and/or biofuel burning (Lai et al. 2010).

1,2-Dichloroethane (11.2 ppt in the plume) was correlated with chloroform (Fig. 4i, $r^2 = 0.64$) and dichloromethane (Fig. 4j, $r^2 = 0.46$), though the correlations were weaker than between dichloromethane and chloroform (Fig. 4k, $r^2 = 0.89$). The moderate correlations could result from the mixture of air masses from different regions or reflect a 1,2-dichloroethane source unrelated to the other two VSLS. To our knowledge, there are no reported measurements of 1,2-dichloroethane from India but there are two reported datasets from Nepal (Adcock et al. 2020; Islam et al. 2020) and multiple studies have reported measurements in China (Barletta et al. 2009; Oram et al. 2017; Xue et al. 2011). Islam et al. (2020) sampled near the center of Kathmandu Valley in April 2015 and reported 1,2-dichloroethane averaged 35.4 ± 23.4 ppt. Adcock et al. (2020) sampled in the upper troposphere and lower stratosphere during the Asian Summer Monsoon over the Indian subcontinent and collected surface measurements at Kathmandu. Adcock et al. (2020) report approximately 10–20 ppt in the tropopause region (θ = 355–375 K) and surface measurements ranged from 10–40 ppt. The POSIDON plume measurements were lower than the Nepal surface mixing ratios and at the low end, but within the range, of Adcock et al. (2020) tropopause measurements. RF05 plume was comparable to Oram et al. (2017) aircraft measurements of 8–12 ppt from 10–12 km over the Bay of Bengal.

Chloroform (12.7 ppt in the plume) was strongly correlated with ethyne (Fig. 4f, $r^2 = 0.92$) suggesting co-location with combustion/industrial sources. Islam et al. (2020) reported an average of 27.6 ± 9.03 ppt at surface sites in Nepal. Adcock et al. (2020) reported ~ 20 ppt in the tropopause region near India. Our POSIDON chloroform results are lower than reported by Adcock et al. (2020) and Islam et al. (2020). However, Oram et al. (2017) reported an average of 7.0 ppt chloroform for flights between Germany and Thailand (10 – 12 km sampling range) with a maximum of 15.6 ppt which is similar to reported here. Approximately 50% of chloroform sources are industrial/anthropogenic (Engel et al. 2018) and the majority (99%) of industrial chloroform produced is for HCFC-22 manufacturing (Say et al. 2019). There was only a weak linear (Fig. 4l, $r^2 = 0.19$) correlation observed between chloroform and HCFC-22 during RF05 that was not statistically significant ($p > 0.05$). Given the different photochemical lifetimes of the two trace gases, a nonlinear correlation in the TTL is expected. For the observed plume during POSIDON, the poor linear correlation results from the relatively small enhancement of HCFC-22 (~ 2.5%) compared to chloroform (60%), and an estimated precision of the HCFC-22 measurement of approximately 1 – 2%. However, the POSIDON HCFC-22 and chloroform correlation is consistent with the larger range of data that were reported in Adcock et al. (2020) for the StratoClim mission adjacent and within the Asian Summer Monsoon. Say et al. (2019) sampled air in the lower troposphere over the Indian subcontinent and data indicate that the HCFC-22 correlation is different over different regions. Sampled areas in West and Northwest India tend to show large, correlated enhancements. The measurements from Northeast India, though, had relatively a larger enhancement of chloroform relative to HCFC-22, which is more consistent with the observations during POSIDON.

Dichloromethane (Δ48.2 ppt) was strongly correlated with ethyne (Fig. 4g, $r^2 = 0.81$). Industrial sources dominate dichloromethane production (Cox et al. 2003; Fang et al. 2019;

Hossaini et al. 2017; Trudinger et al. 2004). Recent studies find dichloromethane mixing ratios similar to our POSIDON plume (~90 ppt). Oram et al. (2017) reported higher dichloromethane measurements over the Bay of Bengal (~70–110 ppt) sampled from 10–12 km. Adcock et al. (2020) found dichloromethane ranged from 65–136 ppt in the tropopause region. Back-trajectories with elevated dichloromethane (>120 ppt) originated in China and along the northwestern portion of the Tibetan Plateau (Adcock et al. 2020). Further, the highest mixing ratios of dichloromethane measured by Say et al. (2019) were in eastern India, near our suggested source region. Islam et al. (2020) reported 103 ± 47.3 ppt at a surface site in Kathmandu. Dichloromethane and chloroform were strongly correlated (Fig. 4k, $r^2 = 0.89$) indicating significant source co-location as found by Say et al. (2019) ($r = 0.71$).

The POSIDON measurements fit into the greater story of chlorinated VSLS measurements in Asia, in particular the Indian subcontinent. Ashford et al. (2015) estimated that transport from the East Asian boundary layer to the tropical upper troposphere could occur in less than 10 days which Oram et al. (2017) supported with aircraft data collected between 10 and 12 km. We show here that these VSLS can be transported to the TTL within 10 days during the transitional period between the summer and winter monsoons.

Air masses in the TTL are expected to be transported to the stratosphere. Chlorinated VSLS still represent a small portion of chlorine in the stratosphere but if emissions continue to rise (e.g. Feng et al. 2018), the stratospheric impact will increase. Engel et al. (2018) estimated 109 ppt Cl in the level of zero radiative heating (LZRH, 355–365 K) from dichloromethane, chloroform, and 1,2-dichloroethane using aircraft data from campaigns in the western Pacific Ocean in 2013 and 2014. LZRH is the region that above that transport to the stratosphere is assumed and a similar potential temperature range as reported here. During POSIDON RF05, the transport of dichloromethane, chloroform, and 1,2-dichloroethane to the western Pacific Ocean TTL potentially added an additional 119 ppt VSL Cl source gas injection into the lower stratosphere, assuming all would be transported to the cold point. The altitude of the Asian Plume event observed during POSIDON was well below the cold point, and elevated mixing ratios of VSLS had decreased to background levels at the cold point tropopause. At temperatures encountered in the TTL, photochemical lifetime of these chlorinated VSLS are quite long, ranging from about 270 – 500 days, so one would predict little degradation over the transit time through the TTL. Thus, while this event was not directly transported to the lower stratosphere, the elevated chlorinated VSL could eventually be transported to the lower stratosphere and contribute to the temporal increase observed for chlorinated VSL at 17 km. For example, we note that dichloromethane at the cold point was approximately 47 ppt during POSIDON, which compares to 32.5 ppt reported in Engel et al. (2018). If we also consider the enhanced methyl halides, then the POSIDON plume represents an additional 197 ppt of equivalent effective chlorine from longer lived halocarbons. Thus, the POSIDON plume transported to the remote TTL over the Western Pacific contains an additional 316 ppt of equivalent chlorine which may enter the lower stratosphere.

3 Conclusion

We present measurements of elevated halocarbon and NMHC mixing ratios sampled in the TTL over the western Pacific Ocean indicative of a continental source with influence from industrial emissions and biofuel/biomass burning. Based on chemical signature and

back-trajectories this air originated from a developing region of Asia, likely India. Particularly important are the elevated chlorinated VSLS measurements relative to the tropical TTL background. This suggests a wide distribution far from sources despite their short lifetime. This is important since the TTL is a major pathway for stratospheric input. The Asian plume reported here had the potential to add an additional 316 ppt equivalent effective chlorine, with 119 ppt from chlorinated VSLS, into the lower stratosphere. This supports recent model work highlighting that as VSLS emissions rise, they have the potential to delay ozone hole recovery time if transported into the lower stratosphere which is possible from the tropical upper troposphere via large-scale ascent.

Supplementary information The online version contains supplementary material available at https://doi.org/10.1007/s10874-022-09430-7.

Acknowledgements We gratefully acknowledge the engineers, technicians, and pilots of National Aeronautics and Space Administration (NASA) Armstrong Flight Research Center, and NASA-ESPO Project Management, and all POSIDON participants. A special thank you to the lead PIs Ru-Shan Gao and Eric Jensen. We thank Richard Lueb and Roger Hendershot for technical support in the field, and Leslie Pope for WAS support. Thanks to Geoff Dutton, Eric Hintsa, and J. David Nance at NOAA/CIRES. This work was supported by NASA Grants NNX13AH20G and NNX17AE43G, and National Science Foundation Grant AGS-1853948. We acknowledge the NOAA Air Resources Laboratory for use of the HYSPLIT model and the NASA EOSDIS for use of the use of imagery from the NASA Worldview application (https://worldview.earthdata.nasa.gov/). POSIDON data is available at https://espoarchive.nasa.gov/archive/browse/posidon.

Funding NASA Grants NNX13AH20G and NNX17AE43G, and NSF Grant AGS-1853948.

Data availability POSIDON data is available at https://espoarchive.nasa.gov/archive/browse/posidon.

Declarations

Conflicts of interest The authors have no conflicts of interests to declare that are relevant to the content of this article.

References

Adcock, K.E., Fraser, P.J., Hall, B.D., Langenfelds, R.L., Lee, G., Montzka, S.A., Oram, D.E., Röckmann, T., Stroh, F., Sturges, W.T., Vogel, B., Laube, J.C.: Aircraft-based observations of ozone-depleting substances in the upper troposphere and lower stratosphere in and above the Asian summer monsoon. J. Geophys. Res. Atmos. (2020). https://doi.org/10.1029/2020JD033137

Andrews, S.J., Carpenter, L.J., Apel, E.C., Atlas, E., Donets, V., Hopkins, J.R., Hornbrook, R.S., Lewis, A.C., Lidster, R.T., Lueb, R., Minaeian, J., Navarro, M., Punjabi, S., Riemer, D., Schauffler, S.: A comparison of very short lived halocarbon (VSLS) and DMS aircraft measurements in the tropical west Pacific from CAST. ATTREX and CONTRAST. Atmos. Meas. Tech. **9**, 5213–5225 (2016). https://doi.org/10.5194/amt-9-5213-2016

Ashfold, M.J., Harris, N.R.P., Atlas, E.L., Manning, A.J., Pyle, J.A.: Transport of short-lived species into the Tropical Tropopause Layer. Atmos. Chem. Phys. **12**, 6309–6322 (2012). https://doi.org/10.5194/acp-12-6309-2012

Ashfold, M.J., Pyle, J.A., Robinson, A.D., Meneguz, E., Nadzir, M.S.M., Phang, S.M., Samah, A.A., Ong, S., Ung, H.E., Peng, L.K., Yong, S.E., Harris, N.R.P.: Rapid transport of East Asian pollution to the deep tropics. Atmos. Chem. Phys. **15**, 3565–3573 (2015). https://doi.org/10.5194/acp-15-3565-2015

Atkinson, R., Baulch, D.L., Cox, R.A., Hampson, R.F., Kerr, J.A., Rossi, M.J., Troe, J.: Evaluated Kinetic, Photochemical and Heterogeneous Data for Atmospheric Chemistry: Supplement V. IUPAC Subcommittee on Gas Kinetic Data Evaluation for Atmospheric Chemistry. J. Phys. Chem. Ref. Data. **26**, 521–1011 (1997). https://doi.org/10.1063/1.556011

Atkinson, R.: Kinetics of the gas-phase reactions of OH radicals with alkanes and cycloalkanes. Atmos. Chem. Phys. **3**, 2233–2307 (2003). https://doi.org/10.5194/acp-3-2233-2003

Baker, A.K., Schuck, T.J., Slemr, F., Van Velthoven, P., Zahn, A., Brenninkmeijer, C.A.M.: Characterization of non-methane hydrocarbons in Asian summer monsoon outflow observed by the CARIBIC aircraft. Atmos. Chem. Phys. **11**, 503–518 (2011). https://doi.org/10.5194/acp-11-503-2011

Barletta, B., Meinardi, S., Simpson, I.J., Atlas, E.L., Beyersdorf, A.J., Baker, A.K., Blake, N.J., Yang, M., Midyett, J.R., Novak, B.J., McKeachie, R.J., Fuelberg, H.E., Sachse, G.W., Avery, M.A., Campos, T., Weinheimer, A.J., Rowland, F.S., Blake, D.R.: Characterization of volatile organic compounds (VOCs) in Asian and north American pollution plumes during INTEX-B: Identification of specific Chinese air mass tracers. Atmos. Chem. Phys. **9**, 5371–5388 (2009). https://doi.org/10.5194/acp-9-5371-2009

Brinckmann, S., Engel, A., Bönisch, H., Quack, B., Atlas, E.: Short-lived brominated hydrocarbons – observations in the source regions and the tropical tropopause layer. Atmos. Chem. Phys. **12**, 1213–1228 (2012). https://doi.org/10.5194/acp-12-1213-2012

Brioude, J., Portmann, R.W., Daniel, J.S., Cooper, O.R., Frost, G.J., Rosenlof, K.H., Granier, C., Ravishankara, A.R., Montzka, S.A., Stohl, A.: Variations in ozone depletion potentials of very short-lived substances with season and emission region. Geophys. Res. Lett. **37**, 3–7 (2010). https://doi.org/10.1029/2010GL044856

Butler, J.H.: Better budgets for methyl halides? Nature **403**, 260–261 (2000). https://doi.org/10.1038/35002232

Claxton, T., Hossaini, R., Wild, O., Chipperfield, M.P., Wilson, C.: On the Regional and Seasonal Ozone Depletion Potential of Chlorinated Very Short-Lived Substances. Geophys. Res. Lett. **46**, 5489–5498 (2019). https://doi.org/10.1029/2018GL081455

Cox, M.L., Sturrock, G.A., Fraser, P.J., Siems, S.T., Krummel, P.B., O'Doherty, S.: Regional sources of methyl chloride, chloroform and dichloromethane identified from AGAGE observations at Cape Grim, Tasmania, 1998–2000. J. Atmos. Chem. **45**, 79–99 (2003). https://doi.org/10.1023/A:1024022320985

Donets, V., Atlas, E.L., Pan, L.L., Schauffler, S.M., Honomichl, S., Hornbrook, R.S., Apel, E.C., Campos, T., Hall, S.R., Ullmann, K., Bresch, J.F., Navarro, M., Blake, D.R.: Wintertime Transport of Reactive Trace Gases From East Asia Into the Deep Tropics. J. Geophys. Res. Atmos. **123**, 12877–12896 (2018). https://doi.org/10.1029/2017JD028231

de Gouw, J.A., Warneke, C., Scheeren, H.A., Van Der Veen, C., Bolder, M., Scheele, M.P., Williams, J., Wong, S., Lange, L., Fischer, H., Lelieveld, J.: Overview of the trace gas measurements on board the Citation aircraft during the intensive field phase of INDOEX. J. Geophys. Res. Atmos. **106**, 28453–28467 (2001). https://doi.org/10.1029/2000JD900810

Engel, A., Rigby, M., Burkholder, J., Fernandez, R.P., Froidevaux, L., Hall, B.D., Hossaini, R., Saito, T., Vollmer, M.K., Yao, B.: Update on Ozone-Depleting Substances (ODSs) and Other Gases of Interest to the Montreal Protocol, Chapter 1 in Scientific Assessment of Ozone Depletion: 2018, Global Ozone Research and Monitoring Project - Report No. 58. , Geneva, Switzerland (2018)

EPA: Draft Scope of the Risk Evaluation for 1,2-Dichloroethane. (2020)

Fang, X., Park, S., Saito, T., Tunnicliffe, R., Ganesan, A.L., Rigby, M., Li, S., Yokouchi, Y., Fraser, P.J., Harth, C.M., Krummel, P.B., Mühle, J., O'Doherty, S., Salameh, P.K., Simmonds, P.G., Weiss, R.F., Young, D., Lunt, M.F., Manning, A.J., Gressent, A., Prinn, R.G.: Rapid increase in ozone-depleting chloroform emissions from China. Nat. Geosci. **12**, 89–93 (2019). https://doi.org/10.1038/s41561-018-0278-2

Feng, Y., Bie, P., Wang, Z., Wang, L., Zhang, J.: Bottom-up anthropogenic dichloromethane emission estimates from China for the period 2005–2016 and predictions of future emissions. Atmos. Environ. **186**, 241–247 (2018). https://doi.org/10.1016/j.atmosenv.2018.05.039

Fiehn, A., Quack, B., Stemmler, I., Ziska, F., Krüger, K.: Importance of seasonally resolved oceanic emissions for bromoform delivery from the tropical Indian Ocean and west Pacific to the stratosphere. Atmos. Chem. Phys. **18**, 11973–11990 (2018). https://doi.org/10.5194/acp-18-11973-2018

Filus, M.T., Atlas, E.L., Navarro, M.A., Meneguz, E., Thomson, D., Ashfold, M.J., Carpenter, L.J., Andrews, S.J., Harris, N.R.P.: Transport of short-lived halocarbons to the stratosphere over the Pacific Ocean. Atmos. Chem. Phys. **20**, 1163–1181 (2020). https://doi.org/10.5194/acp-20-1163-2020

Flocke, F., Herman, R.L., Salawitch, R.J., Atlas, E., Webster, C.R., Schauffler, S.M., Lueb, R.A., May, R.D., Moyer, E.J., Rosenlof, K.H., Scott, D.C., Blake, D.R., Bui, T.P.: An examination of chemistry and transport processes in the tropical lower stratosphere using observations of long-lived and short-lived compounds obtained during STRAT and POLARIS. J. Geophys. Res. Atmos. **104**, 26625–26642 (1999). https://doi.org/10.1029/1999JD900504

Fueglistaler, S., Dessler, A.E., Dunkerton, T.J., Folkins, I., Fu, Q., Mote, P.W.: Tropical tropopause layer. Rev. Geophys. **47**, 1–31 (2009). https://doi.org/10.1029/2008RG000267

Fuhlbrügge, S., Quack, B., Tegtmeier, S., Atlas, E., Hepach, H., Shi, Q., Raimund, S., Krüger, K.: The contribution of oceanic halocarbons to marine and free tropospheric air over the tropical West Pacific. Atmos. Chem. Phys. **16**, 7569–7585 (2016). https://doi.org/10.5194/acp-16-7569-2016

Gao, R.S., Ballard, J., Watts, L.A., Thornberry, T.D., Ciciora, S.J., McLaughlin, R.J., Fahey, D.W.: A compact, fast UV photometer for measurement of ozone from research aircraft. Atmos. Meas. Tech. **5**, 2201–2210 (2012). https://doi.org/10.5194/amt-5-2201-2012

Guo, H., Wang, T., Simpson, I.J., Blake, D.R., Yu, X.M., Kwok, Y.H., Li, Y.S.: Source contributions to ambient VOCs and CO at a rural site in eastern China. Atmos. Environ. **38**, 4551–4560 (2004). https://doi.org/10.1016/j.atmosenv.2004.05.004

Hall, B.D., Engel, A., Mühle, J., Elkins, J.W., Artuso, F., Atlas, E., Aydin, M., Blake, D., Brunke, E.G., Chiavarini, S., Fraser, P.J., Happell, J., Krummel, P.B., Levin, I., Loewenstein, M., Maione, M., Montzka, S.A., O'Doherty, S., Reimann, S., Rhoderick, G., Saltzman, E.S., Scheel, H.E., Steele, L.P., Vollmer, M.K., Weiss, R.F., Worthy, D., Yokouchi, Y.: Results from the International Halocarbons in Air Comparison Experiment (IHALACE). Atmos. Meas. Tech. **7**, 469–490 (2014). https://doi.org/10.5194/amt-7-469-2014

Hossaini, R., Atlas, E., Dhomse, S.S., Chipperfield, M.P., Bernath, P.F., Fernando, A.M., Mühle, J., Leeson, A.A., Montzka, S.A., Feng, W., Harrison, J.J., Krummel, P., Vollmer, M.K., Reimann, S., O'Doherty, S., Young, D., Maione, M., Arduini, J., Lunder, C.R.: Recent Trends in Stratospheric Chlorine From Very Short-Lived Substances. J. Geophys. Res. Atmos. **124**, 2318–2335 (2019). https://doi.org/10.1029/2018JD029400

Hossaini, R., Chipperfield, M.P., Montzka, S.A., Leeson, A.A., Dhomse, S.S., Pyle, J.A.: The increasing threat to stratospheric ozone from dichloromethane. Nat. Commun. **8**, 1–9 (2017). https://doi.org/10.1038/ncomms15962

Islam, M.R., Jayarathne, T., Simpson, I.J., Werden, B., Maben, J., Gilbert, A., Praveen, P.S., Adhikari, S., Panday, A.K., Rupakheti, M., Blake, D.R., Yokelson, R.J., Decarlo, P.F., Keene, W.C., Stone, E.A.: Ambient air quality in the Kathmandu Valley, Nepal, during the pre-monsoon: Concentrations and sources of particulate matter and trace gases. Atmos. Chem. Phys. **20**, 2927–2951 (2020). https://doi.org/10.5194/acp-20-2927-2020

Kim, J., Joan Alexander, M.: A new wave scheme for trajectory simulations of stratospheric water vapor. Geophys. Res. Lett. **40**, 5286–5290 (2013). https://doi.org/10.1002/grl.50963

Krüger, K., Quack, B.: Introduction to special issue: The transbrom sonne expedition in the tropical west pacific. Atmos. Chem. Phys. **13**, 9439–9446 (2013). https://doi.org/10.5194/acp-13-9439-2013

Lai, S.C., Baker, A.K., Schuck, T.J., Van Velthoven, P., Oram, D.E., Zahn, A., Hermann, M., Weigelt, A., Slemr, F., M. Brenninkmeijer, C.A., Ziereis, H.: Pollution events observed during CARIBIC flights in the upper troposphere between South China and the Philippines. Atmos. Chem. Phys. **10**, 1649–1660 (2010). https://doi.org/10.5194/acp-10-1649-2010

Lal, S., Sahu, L.K., Venkataramani, S., Mallik, C.: Light non-methane hydrocarbons at two sites in the Indo-Gangetic Plain. J. Environ. Monit. **14**, 1159–1166 (2012). https://doi.org/10.1039/c2em10682e

Lelieveld, J., Gromov, S., Pozzer, A., Taraborrelli, D.: Global tropospheric hydroxyl distribution, budget and reactivity. Atmos. Chem. Phys. **16**, 12477–12493 (2016). https://doi.org/10.5194/acp-16-12477-2016

Levine, J.G., Braesicke, P., Harris, N.R.P., Savage, N.H., Pyle, J.A.: Pathways and timescales for troposphere-to-stratosphere transport via the tropical tropopause layer and their relevance for very short lived substances. J. Geophys. Res. **112**, D04308 (2007). https://doi.org/10.1029/2005JD006940

Liu, Y., Yvon-Lewis, S.A., Hu, L., Salisbury, J.E., O'Hern, J.E.: CHBr3 , CH2Br2 , and CHClBr2 in U.S. coastal waters during the Gulf of Mexico and East Coast Carbon cruise. J. Geophys. Res. **116**, C10004 (2011). https://doi.org/10.1029/2010JC006729

Mallik, C., Ghosh, D., Ghosh, D., Sarkar, U., Lal, S., Venkataramani, S.: Variability of SO2, CO, and light hydrocarbons over a megacity in Eastern India: Effects of emissions and transport. Environ. Sci. Pollut. Res. **21**, 8692–8706 (2014). https://doi.org/10.1007/s11356-014-2795-x

Manö, S., Andreae, M.O.: Emission of methyl bromide from biomass burning. Science (80-.). **263**, 1255–1257 (1994). https://doi.org/10.1126/science.263.5151.1255

Montzka, S.A., Reimannander, S., Engel, A., Kruger, K., Simon, O., Sturges, W.T., Blake, D.R., Dorf, M.D., Fraser, P.J., Froidevaux, L., Jucks, K., Kreher, K., Kurylo III, M.J., Mellouki, A., Jo, D.P.V.: Chapter 1: Ozone-depleting Substances (ODSs) and Related Chemicals. In: Scientific Assessment of Ozone Depletion: 2010,Global Ozone Research and Monitoring Project-Report No.52 (2011)

Oram, D.E., Ashfold, M.J., Laube, J.C., Gooch, L.J., Humphrey, S., Sturges, W.T., Leedham-Elvidge, E., Forster, G.L., Harris, N.R.P., Iqbal Mead, M., Samah, A.A., Phang, S.M., Ou-Yang, C.F., Lin, N.H., Wang, J.L., Baker, A.K., Brenninkmeijer, C.A.M., Sherry, D.: A growing threat to the ozone layer from short-lived anthropogenic chlorocarbons. Atmos. Chem. Phys. **17**, 11929–11941 (2017). https://doi.org/10.5194/acp-17-11929-2017

Orbe, C., Waugh, D.W., Newman, P.A.: Air-mass origin in the tropical lower stratosphere: The influence of Asian boundary layer air. Geophys. Res. Lett. **42**, 4240–4248 (2015). https://doi.org/10.1002/2015GL063937

Pfister, L., Selkirk, H.B., Starr, D.O., Rosenlof, K., Newman, P.A.: A meteorological overview of the TC4 mission. J. Geophys. Res. Atmos. **115**, 1–24 (2010). https://doi.org/10.1029/2009JD013316

Pisso, I., Haynes, P.H., Law, K.S.: Emission location dependent ozone depletion potentials for very short-lived halogenated species. Atmos. Chem. Phys. **10**, 12025–12036 (2010). https://doi.org/10.5194/acp-10-12025-2010

Prinn, R.G., Weiss, R.F., Arduini, J., Arnold, T., DeWitt, H.L., Fraser, P.J., Ganesan, A.L., Gasore, J., Harth, C.M., Hermansen, O., Kim, J., Krummel, P.B., Li, S., Loh, Z.M., Lunder, C.R., Maione, M., Manning, A.J., Miller, B.R., Mitrevski, B., Mühle, J., O'Doherty, S., Park, S., Reimann, S., Rigby, M., Saito, T., Salameh, P.K., Schmidt, R., Simmonds, P.G., Steele, L.P., Vollmer, M.K., Wang, R.H., Yao, B., Yokouchi, Y., Young, D., Zhou, L.: History of chemically and radiatively important atmospheric gases from the Advanced Global Atmospheric Gases Experiment (AGAGE). Earth Syst. Sci. Data. **10**, 985–1018 (2018). https://doi.org/10.5194/essd-10-985-2018

Quack, B., Atlas, E., Petrick, G., Wallace, D.W.R.: Bromoform and dibromomethane above the Mauritanian upwelling: Atmospheric distributions and oceanic emissions. J. Geophys. Res. **112**, D09312 (2007). https://doi.org/10.1029/2006JD007614

Rex, M., Wohltmann, I., Ridder, T., Lehmann, R., Rosenlof, K., Wennberg, P., Weisenstein, D., Notholt, J., Krüger, K., Mohr, V., Tegtmeier, S.: A tropical West Pacific OH minimum and implications for stratospheric composition. Atmos. Chem. Phys. **14**, 4827–4841 (2014). https://doi.org/10.5194/acp-14-4827-2014

Rollins, A.W., Thornberry, T.D., Atlas, E., Navarro, M., Schauffler, S., Moore, F., Elkins, J.W., Ray, E., Rosenlof, K., Aquila, V., Gao, R.S.: SO2 Observations and Sources in the Western Pacific Tropical Tropopause Region. J. Geophys. Res. Atmos. **123**, 13549–13559 (2018). https://doi.org/10.1029/2018JD029635

Rollins, A.W., Thornberry, T.D., Ciciora, S.J., McLaughlin, R.J., Watts, L.A., Hanisco, T.F., Baumann, E., Giorgetta, F.R., Bui, T.V., Fahey, D.W., Gao, R.-S.: A laser-induced fluorescence instrument for aircraft measurements of sulfur dioxide in the upper troposphere and lower stratosphere. Atmos. Meas. Tech. **9**, 4601–4613 (2016). https://doi.org/10.5194/amt-9-4601-2016

Rudolph, J., Khedim, A., Koppmann, R., Bonsang, B.: Field study of the emissions of methyl chloride and other halocarbons from biomass burning in Western Africa. J. Atmos. Chem. **22**, 67–80 (1995). https://doi.org/10.1007/BF00708182

Sahu, L.K., Lal, S., Venkataramani, S.: Distributions of O3, CO and hydrocarbons over the Bay of Bengal: A study to assess the role of transport from southern India and marine regions during September-October 2002. Atmos. Environ. **40**, 4633–4645 (2006). https://doi.org/10.1016/j.atmosenv.2006.02.037

Santee, M.L., Livesey, N.J., Manney, G.L., Lambert, A., Read, W.G.: Methyl chloride from the Aura Microwave Limb Sounder: First global climatology and assessment of variability in the upper troposphere and stratosphere. J. Geophys. Res. Atmos. **118**, 13532–13560 (2013). https://doi.org/10.1002/2013JD020235

Sarangi, T., Naja, M., Lal, S., Venkataramani, S., Bhardwaj, P., Ojha, N., Kumar, R., Chandola, H.C.: First observations of light non-methane hydrocarbons (C2-C5) over a high altitude site in the central Himalayas. Atmos. Environ. **125**, 450–460 (2016). https://doi.org/10.1016/j.atmosenv.2015.10.024

Say, D., Ganesan, A.L., Lunt, M.F., Rigby, M., O'Doherty, S., Harth, C., Manning, A.J., Krummel, P.B., Bauguitte, S.: Emissions of halocarbons from India inferred through atmospheric measurements. Atmos. Chem. Phys. **19**, 9865–9885 (2019). https://doi.org/10.5194/acp-19-9865-2019

Schauffler, S.M., Atlas, E.L., Blake, D.R., Flocke, F., Lueb, R.A., Lee-Taylor, J.M., Stroud, V., Travnicek, W.: Distributions of brominated organic compounds in the troposphere and lower stratosphere. J. Geophys. Res. Atmos. **104**, 21513–21535 (1999). https://doi.org/10.1029/1999JD900197

Scheeren, H.A., Lelieveld, J., De Gouw, J.A., Van Der Veen, C., Fischer, H.: Methyl chloride and other chlorocarbons in polluted air during INDOEX. J. Geophys. Res. Atmos. **107**, (2002). https://doi.org/10.1029/2001JD001121

Schoeberl, M.R., Jensen, E.J., Pfister, L., Ueyama, R., Avery, M., Dessler, A.E.: Convective Hydration of the Upper Troposphere and Lower Stratosphere. J. Geophys. Res. Atmos. **123**, 4583–4593 (2018). https://doi.org/10.1029/2018JD028286

Sherwood, S.C., Chae, J.-H., Minnis, P., McGill, M.: Underestimation of deep convective cloud tops by thermal imagery. Geophys. Res. Lett. **31**, L11102 (2004). https://doi.org/10.1029/2004GL019699

Simmonds, P.G., Manning, A.J., Cunnold, D.M., McCulloch, A., O'Doherty, S., Derwent, R.G., Krummel, P.B., Fraser, P.J., Dunse, B., Porter, L.W., Wang, R.H.J., Greally, B.R., Miller, B.R., Salameh, P., Weiss, R.F., Prinn, R.G.: Global trends, seasonal cycles, and European emissions of dichloromethane, trichloroethene,

and tetrachloroethene from the AGAGE observations at Mace Head, Ireland and Cape Grim. Tasmania. J. Geophys. Res. Atmos. **111**, 1–19 (2006). https://doi.org/10.1029/2006JD007082

Simpson, I.J., Akagi, S.K., Barletta, B., Blake, N.J., Choi, Y., Diskin, G.S., Fried, A., Fuelberg, H.E., Meinardi, S., Rowland, F.S., Vay, S.A., Weinheimer, A.J., Wennberg, P.O., Wiebring, P., Wisthaler, A., Yang, M., Yokelson, R.J., Blake, D.R.: Boreal forest fire emissions in fresh Canadian smoke plumes: C1–C10 volatile organic compounds (VOCs), CO2, CO, NO2, NO, HCN and CH3CN. Atmos. Chem. Phys. **11**, 6445–6463 (2011). https://doi.org/10.5194/acp-11-6445-2011

Solomon, S., Albritton, D.L.: Time-dependent ozone depletion potentials for short- and long-term forecasts. Nature **357**, 33–37 (1992). https://doi.org/10.1038/357033a0

Tang, J.H., Chan, L.Y., Chang, C.C., Liu, S., Li, Y.S.: Characteristics and sources of non-methane hydrocarbons in background atmospheres of eastern, southwestern, and southern China. J. Geophys. Res. Atmos. **114**, (2009). https://doi.org/10.1029/2008JD010333

Tegtmeier, S., Atlas, E., Quack, B., Ziska, F., Krüger, K.: Variability and past long-term changes of brominated very short-lived substances at the tropical tropopause. Atmos. Chem. Phys. **20**, 7103–7123 (2020). https://doi.org/10.5194/acp-20-7103-2020

Tegtmeier, S., Krüger, K., Quack, B., Atlas, E., Blake, D.R., Boenisch, H., Engel, A., Hepach, H., Hossaini, R., Navarro, M.A., Raimund, S., Sala, S., Shi, Q., Ziska, F.: The contribution of oceanic methyl iodide to stratospheric iodine. Atmos. Chem. Phys. **13**, 11869–11886 (2013). https://doi.org/10.5194/acp-13-11869-2013

Tegtmeier, S., Krüger, K., Quack, B., Atlas, E.L., Pisso, I., Stohl, A., Yang, X.: Emission and transport of bromocarbons: From the West Pacific ocean into the stratosphere. Atmos. Chem. Phys. **12**, 10633–10648 (2012). https://doi.org/10.5194/acp-12-10633-2012

Trudinger, C.M., Etheridge, D.M., Sturrock, G.A., Fraser, P.J., Krummel, P.B., McCulloch, A.: Atmospheric histories of halocarbons from analysis of Antarctic firn air: Methyl bromide, methyl chloride, chloroform, and dichloromethane. J. Geophys. Res. D Atmos. **109**, 1–15 (2004). https://doi.org/10.1029/2004JD004932

Ueyama, R., Jensen, E.J., Pfister, L.: Convective Influence on the Humidity and Clouds in the Tropical Tropopause Layer During Boreal Summer. J. Geophys. Res. Atmos. **123**, (2018). https://doi.org/10.1029/2018JD028674

Ueyama, R., Jensen, E.J., Pfister, L., Kim, J.: Dynamical, convective, and microphysical control on wintertime distributions of water vapor and clouds in the tropical tropopause layer. J. Geophys. Res. Atmos. **120**, 2689–2705 (2015). https://doi.org/10.1002/2015JD023318

Umezawa, T., Baker, A.K., Oram, D., Sauvage, C., O'Sullivan, D., Rauthe-Schöch, A., Montzka, S.A., Zahn, A., Brenninkmeijer, C.A.M.: Methyl chloride in the upper troposphere observed by the CARIBIC passenger aircraft observatory: Large-scale distributions and Asian summer monsoon outflow. J. Geophys. Res. Atmos. **119**, 5542–5558 (2014). https://doi.org/10.1002/2013JD021396

Vogel, B., Müller, R., Günther, G., Spang, R., Hanumanthu, S., Li, D., Riese, M., Stiller, G.P.: Lagrangian simulations of the transport of young air masses to the top of the Asian monsoon anticyclone and into the tropical pipe. Atmos. Chem. Phys. **19**, 6007–6034 (2019). https://doi.org/10.5194/acp-19-6007-2019

Warwick, N.J., Pyle, J.A., Shallcross, D.E.: Global modelling of the atmospheric methyl bromide budget. J. Atmos. Chem. **54**, 133–159 (2006). https://doi.org/10.1007/s10874-006-9020-3

Wofsy, S.C.: HIAPER Pole-to-Pole Observations (HIPPO): fine-grained, global-scale measurements of climatically important atmospheric gases and aerosols. Philos. Trans. R. Soc. A Math. Phys. Eng. Sci. **369**, 2073–2086 (2011). https://doi.org/10.1098/rsta.2010.0313

Wuebbles, D.J., Luther, F.M., Penner, J.E.: Effect of coupled anthropogenic perturbations on stratospheric ozone. J. Geophys. Res. **88**, 1444 (1983). https://doi.org/10.1029/JC088iC02p01444

Xue, L., Wang, T., Simpson, I.J., Ding, A., Gao, J., Blake, D.R., Wang, X., Wang, W., Lei, H., Jin, D.: Vertical distributions of non-methane hydrocarbons and halocarbons in the lower troposphere over northeast China. Atmos. Environ. **45**, 6501–6509 (2011). https://doi.org/10.1016/j.atmosenv.2011.08.072

Yates, E.L., Derwent, R.G., Simmonds, P.G., Greally, B.R., O'Doherty, S., Shallcross, D.E.: The seasonal cycles and photochemistry of C2–C5 alkanes at Mace Head. Atmos. Environ. **44**, 2705–2713 (2010). https://doi.org/10.1016/j.atmosenv.2010.04.043

Authors and Affiliations

Victoria Treadaway[1] · Elliot Atlas[1] · Sue Schauffler[2] · Maria Navarro[1] · Rei Ueyama[3] · Leonhard Pfister[3] · Troy Thornberry[4] · Andrew Rollins[4] · James Elkins[5] · Fred Moore[5] · Karen Rosenlof[4]

Elliot Atlas
eatlas@miami.edu

1 Department of Atmospheric Sciences, Rosenstiel School of Marine and Atmospheric Science, University of Miami, Miami, FL, USA

2 Atmospheric Chemistry Observations and Modeling Laboratory, National Center for Atmospheric Research, Boulder, CO, USA

3 NASA Ames Research Center, Moffett Field, CA, USA

4 NOAA Chemical Sciences Laboratory, Boulder, CO, USA

5 NOAA Global Monitoring Laboratory, Boulder, CO, USA